

# Design and Analysis of a Robust Control System for Triple Inverted Pendulum Stabilization

Tohid Kargar Tasooji, Sakineh Khodadadi

**Abstract**—The design of robust controllers for triple inverted pendulum systems presents significant challenges due to their inherent instability and nonlinear dynamics. Moreover, uncertainties in system parameters further complicate the control design. This paper investigates a robust control strategy for triple inverted pendulums under parameter uncertainty. Two control approaches, namely the  $H_\infty$  controller and the  $\mu$ -synthesis controller, are compared in terms of their ability to achieve reference tracking and disturbance rejection. Simulation results demonstrate that the  $H_\infty$  controller provides superior transient performance, making it a promising solution for robust stabilization of such complex systems.

**Index Terms**—Robust control, triple inverted pendulum,  $H_\infty$  control,  $\mu$ -synthesis, nonlinear systems.

## I. INTRODUCTION

In control theory, standard benchmark systems play a pivotal role in validating new methods and theories, with the inverted pendulum being one of the most widely used due to its structural simplicity and inherent instability [1]. As a fundamental example of an underactuated mechanical system, the inverted pendulum has proven valuable for both research and education in nonlinear control. In particular, the triple-link inverted pendulum system (TIPS) exhibits highly nonlinear, high-order, multivariable, and unstable dynamics that mirror challenges encountered in flexible space structures, bipedal robotic locomotion, and automatic aircraft landing systems [2]. Consequently, a wide array of control strategies—from classical to robust and adaptive techniques—have been investigated to stabilize TIPS [3], [4].

Recent advances in event-triggered control have improved the stabilization of complex systems, including multi-agent coordination and secure control under cyber attacks [7]–[11]. By reducing control updates while ensuring stability, these mechanisms are well-suited for real-time, resource-constrained environments [8]–[10]. Decentralized control strategies, such as cooperative localization, offer scalable solutions for handling uncertainties [7], [11]. These methods have been applied in vehicular platooning [33], renewable energy systems [14], [15], and actuator torque control [16]. Additionally, model predictive control (MPC) effectively manages nonlinearities and constraints, ensuring optimal performance [21].

These innovative control approaches have also inspired significant efforts toward stabilizing the Triple Inverted Pendulum System (TIPS). For example, robust servo controllers for a triple inverted pendulum utilizing two independent motors

have been developed, where the bottom link is hinged to the ground and fixed horizontal bars increase inertia to simplify the control challenge [3]. More complex configurations, such as a TIPS mounted on a cart driven by dual DC motors, have also been explored; one motor moves the cart while the other controls the motion of the third arm, adding further dynamic complexity [4]. Moreover, advanced robust control frameworks, including the  $H_\infty$  approach using both dynamic and static state feedback methods, have been investigated to enhance system robustness in the face of uncertainties and external disturbances, which are critical in high-dimensional nonlinear systems like TIPS [5].

The main contributions of this paper are summarized as follows:

- 1) We propose a robust control strategy for the Triple Inverted Pendulum System (TIPS) that explicitly accounts for system uncertainties and nonlinear dynamics. The control framework is developed using both  $H_\infty$  and  $\mu$ -synthesis techniques to ensure robust performance under varying operating conditions.
- 2) A comprehensive comparison between the  $H_\infty$  controller and the  $\mu$ -synthesis controller is provided. This includes an in-depth analysis of reference tracking, disturbance rejection capabilities, and transient response characteristics under a range of realistic scenarios.
- 3) Detailed simulation studies are conducted to validate the proposed control methodologies. The results demonstrate that the  $H_\infty$  controller outperforms its  $\mu$ -synthesis counterpart in terms of transient response, thus offering a promising solution for the robust stabilization of TIPS.
- 4) The insights gained from the robust control design and simulation studies extend beyond the TIPS, offering valuable perspectives applicable to other complex, under-actuated, and nonlinear systems encountered in industrial and aerospace applications.

The remainder of this paper is organized as follows. Section II describes the system dynamics, including the mathematical modeling of the triple inverted pendulum using Lagrange's equations. Section III presents the proposed robust control strategies, detailing the  $H_\infty$  controller and the  $\mu$ -synthesis approach. Section IV provides a comparative analysis of the controllers, evaluating their performance in terms of reference tracking, disturbance rejection, and transient response characteristics. Section V discusses the simulation results and their implications for real-world applications. Finally, Section VI concludes the paper with key findings and future research directions.

Tohid Kargar Tasooji is with the Department of Aerospace Engineering, Toronto Metropolitan University, Toronto, ON M5B 2K3, Canada (e-mail: tohid.kargartasooji@torontomu.ca). Sakineh Khodadadi is with the Department of Electrical and Computer Engineering, University of Alberta, Edmonton, AB, AB T6G 1H9, Canada (email: sakineh@ualberta.ca).

## II. SYSTEM DESCRIPTION

The triple inverted pendulum considered in this work is based on the experimental setup realized by Furuta et al. [6]. The pendulum consists of three arms connected by ball-bearing hinges that allow rotation in the vertical plane. The torques at the two upper hinges are controlled by DC motors, while the lowest hinge is free to rotate. By regulating the angles of the two upper arms about specified setpoints, the pendulum can be stabilized in the inverted configuration. To facilitate control, a horizontal bar is attached to each arm to increase the moment of inertia. Two DC motors, denoted by  $M_1$  and  $M_2$ , are mounted on the first and third arms, respectively, and deliver torques via timing belts. Potentiometers  $P_1$ ,  $P_2$ , and  $P_3$  are fixed at the hinges to measure the corresponding angles.

The pendulum model is derived using Lagrange's equations [6] and is expressed by the following nonlinear vector-matrix differential equation:

$$M(\boldsymbol{\theta})\ddot{\boldsymbol{\theta}} + N(\boldsymbol{\theta})\dot{\boldsymbol{\theta}} + \mathbf{q}(\boldsymbol{\theta}) + G_m \begin{bmatrix} tm_1 \\ tm_2 \end{bmatrix} = T \begin{bmatrix} \delta_1 \\ \delta_2 \\ \delta_3 \end{bmatrix}, \quad (1)$$

where  $\boldsymbol{\theta} = [\theta_1 \ \theta_2 \ \theta_3]^T$  is the vector of joint angles. The matrices and vectors in (1) are defined as follows.

The mass matrix is given by

$$M(\boldsymbol{\theta}) = \begin{bmatrix} J_1 + I_{p1} & l_1 M_2 \cos(\theta_1 - \theta_2) - I_{p1} & l_1 M_3 \cos(\theta_1 - \theta_3) \\ l_1 M_2 \cos(\theta_1 - \theta_2) - I_{p1} & J_2 + I_{p1} + I_{p2} & l_2 M_3 \cos(\theta_2 - \theta_3) - I_{p2} \\ l_1 M_3 \cos(\theta_1 - \theta_3) & l_2 M_3 \cos(\theta_2 - \theta_3) - I_{p2} & J_3 + I_{p2} \end{bmatrix} \quad (2)$$

The damping matrix is expressed as

$$N(\boldsymbol{\theta}) = \begin{bmatrix} C_1 + C_2 + C_{p1} & -C_2 - C_{p1} & 0 \\ -C_2 - C_{p1} & C_{p1} + C_{p2} + C_2 + C_3 & -C_3 - C_{p2} \\ 0 & -C_3 - C_{p2} & C_3 + C_{p2} \end{bmatrix} \quad (3)$$

The transformation matrix  $T$  and gain matrix  $K$  are given by

$$T = \begin{bmatrix} 1 & -1 & 0 \\ 0 & 1 & -1 \\ 0 & 0 & 1 \end{bmatrix}, \quad K = \begin{bmatrix} K_1 & 0 \\ -K_1 & K_2 \\ 0 & -K_2 \end{bmatrix}. \quad (4)$$

The vector  $\mathbf{q}(\boldsymbol{\theta})$  capturing gravitational and nonlinear inertial effects is defined as

$$\begin{aligned} q_1 &= l_1 M_2 \sin(\theta_1 - \theta_2) \dot{\theta}_2^2 + l_1 M_3 \sin(\theta_1 - \theta_3) \dot{\theta}_3^2 - M_1 g \sin(\theta_1), \\ q_2 &= l_1 M_2 \sin(\theta_1 - \theta_2) \dot{\theta}_1^2 + l_2 M_3 \sin(\theta_2 - \theta_3) \dot{\theta}_3^2 - M_2 g \sin(\theta_2), \\ q_3 &= l_1 M_3 \sin(\theta_1 - \theta_3) (\dot{\theta}_1^2 - 2\dot{\theta}_1 \dot{\theta}_3) + l_2 M_3 \sin(\theta_2 - \theta_3) (\dot{\theta}_2^2 - 2\dot{\theta}_2 \dot{\theta}_3) - M_3 g \sin(\theta_3). \end{aligned} \quad (5)$$

Additional parameter definitions are given by

$$\begin{aligned} C_{p_i} &= C_{p0_i} + K_2 C_{m_i}, \quad I_{p_i} = I_{p0_i} + K_2 I_{m_i}, \\ M_1 &= m_1 h_1 + m_2 l_1 + m_3 l_1, \quad M_2 = m_2 h_2 + m_3 l_2, \quad M_3 = m_3 h_3, \\ J_1 &= I_1 + m_1 h_1^2 + m_2 l_1^2 + m_3 l_1^2, \quad J_2 = I_2 + m_2 h_2^2 + m_3 l_2^2, \quad J_3 = I_3 + m_3 h_3^2. \end{aligned} \quad (6)$$

All other parameters and variables are defined in Table I.

By linearizing the nonlinear model under the assumptions of small angular deviations from the vertical and low velocities, the linearized model is expressed as

$$M \ddot{\boldsymbol{\theta}} + N \dot{\boldsymbol{\theta}} + P \boldsymbol{\theta} + G_m \begin{bmatrix} tm_1 \\ tm_2 \end{bmatrix} = T \begin{bmatrix} \delta_1 \\ \delta_2 \\ \delta_3 \end{bmatrix}, \quad (7)$$

where the linear mass matrix is

$$M = \begin{bmatrix} J_1 + I_{p1} & l_1 M_2 - I_{p1} & l_1 M_3 \\ l_1 M_2 - I_{p1} & J_2 + I_{p1} + I_{p2} & l_2 M_3 - I_{p2} \\ l_1 M_3 & l_2 M_3 - I_{p2} & J_3 + I_{p2} \end{bmatrix}, \quad (8)$$

and the stiffness matrix is

$$P = \begin{bmatrix} M_1 g & 0 & 0 \\ 0 & M_2 g & 0 \\ 0 & 0 & M_3 g \end{bmatrix}. \quad (9)$$

In (10), the vector  $tm = [tm_1 \ tm_2]^T$  represents the control torques,  $d = [\delta_1 \ \delta_2 \ \delta_3]^T$  is the disturbance torque vector, and  $y = [\theta_1 \ \theta_2 \ \theta_3]^T$  is the output vector.

The outputs are measured by linear potentiometers, whose voltages are given by

$$y_{p1} = \beta_1 \theta_1, \quad y_{p2} = \beta_2 (\theta_2 - \theta_1), \quad y_{p3} = \beta_3 (\theta_3 - \theta_2). \quad (10)$$

### A. Modeling of Uncertainties

In practice, some parameters may vary due to environmental factors such as temperature. In this work, the moments of inertia  $I_1$ ,  $I_2$ , and  $I_3$  of the three arms, along with the viscous friction coefficients  $C_1$ ,  $C_2$ ,  $C_3$ ,  $C_{m1}$ , and  $C_{m2}$ , are considered as uncertainty parameters. Accounting for these uncertainties, the matrices  $M$  and  $N$  in the linearized pendulum model are recomputed. In addition, unmodeled dynamics and nonlinear effects in the actuator models are represented by input multiplicative uncertainties:

$$G_{m1} = (1 + W_{m1} \Delta_{m1}) \tilde{G}_{m1}, \quad (11)$$

$$G_{m2} = (1 + W_{m2} \Delta_{m2}) \tilde{G}_{m2}, \quad (12)$$

where  $|\Delta_{m1}| < 1$  and  $|\Delta_{m2}| < 1$ . The uncertainty weights  $W_{m1}$  and  $W_{m2}$  are selected such that

$$\begin{aligned} \left\| \frac{G_{m1}(j\omega) - \tilde{G}_{m1}(j\omega)}{\tilde{G}_{m1}(j\omega)} \right\| &< \|W_{m1}(j\omega)\|, \\ \left\| \frac{G_{m2}(j\omega) - \tilde{G}_{m2}(j\omega)}{\tilde{G}_{m2}(j\omega)} \right\| &< \|W_{m2}(j\omega)\|. \end{aligned} \quad (13)$$

### B. $H_\infty$ Design

An  $H_\infty$  sub-optimal control law is designed for the configuration illustrated in Fig. 2. In this framework, the variable  $G$  denotes the nominal transfer function matrix,  $G_{\text{nom}}$ , of the augmented plant. The objective of the  $H_\infty$  control design is to minimize the  $k : k_1$  norm of the closed-loop transfer function

$$S(G_{\text{nom}}; K),$$

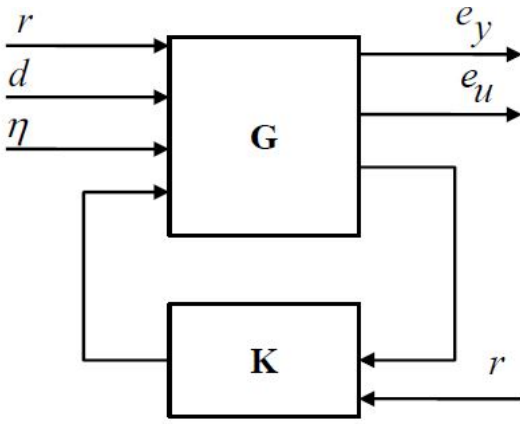


Fig. 1: Block diagram of linear fractional transformation

which characterizes the mapping from the exogenous inputs—comprising reference signals, disturbances, and measurement noise—to the weighted performance outputs,  $e_u$  and  $e_y$ . Here,  $K$  represents the set of all controllers that stabilize the augmented system.

The design procedure involves iteratively adjusting the parameter  $\gamma$ , which serves as an upper bound on the  $H_\infty$  norm of the closed-loop transfer function. This iterative process is continued until the minimal achievable  $H_\infty$  norm is obtained, ensuring that the controller not only stabilizes the system but also achieves the desired level of performance in terms of disturbance rejection and reference tracking.

For the synthesis of the  $H_\infty$  controller, the MATLAB function `hinfsyn` is utilized. This function computes a controller  $K$  that minimizes the worst-case gain from the disturbance inputs to the performance outputs, subject to the constraint that the closed-loop system remains stable. The resulting controller is thus robust against uncertainties and external disturbances, fulfilling the design criteria for high-performance control of the augmented system.

### C. $\mu$ -Synthesis

In this section, a  $\mu$  controller is designed to analyze the transient response of the closed-loop system. To capture the various uncertainties present in the system, we define a block-diagonal uncertainty matrix  $\Delta_p$  as follows:

$$\Delta_p = \begin{bmatrix} \Delta & 0 \\ 0 & \Delta_F \end{bmatrix}, \quad \Delta \in \mathbb{R}^{10 \times 10}, \quad \Delta_F \in \mathbb{C}^{9 \times 5}. \quad (14)$$

The first block,  $\Delta$ , corresponds to the parametric and linear time-invariant uncertainties modeled in the triple inverted pendulum system. The second block,  $\Delta_F$ , is a fictitious uncertainty introduced to incorporate performance objectives within the  $\mu$ -synthesis framework. The inputs to  $\Delta_F$  are the weighted error signals  $e_y$  and  $e_u$ , and its outputs consist of the exogenous inputs  $r$ ,  $d$ , and additional uncertainty signals.

The objective of the  $\mu$  controller is to design a stabilizing controller  $K$  such that, for each frequency  $\omega \in [0, 1]$ , the structured singular value satisfies

$$\mu_{\Delta_p}(F_L(P, K)(j\omega)) < 1, \quad (15)$$

TABLE I: Parameters and Variables Definition

Parameter	Description	Value
$l_1$ (m)	Length of the 1st arm	0.5
$l_2$ (m)	Length of the 2nd arm	0.4
$h_1$ (m)	Distance from bottom to the center of gravity of the 1st arm	0.35
$h_2$ (m)	Distance from bottom to the center of gravity of the 2nd arm	0.181
$h_3$ (m)	Distance from bottom to center of gravity of the 3rd arm	0.245
$m_1$ (kg)	Mass of the 1st arm	3.25
$m_2$ (kg)	Mass of the 2nd arm	1.90
$m_3$ (kg)	Mass of the 3rd arm	2.23
$I_1$ (kg:m <sup>2</sup> )	Moment of inertia of the 1st arm around the center of gravity	0.654
$I_2$ (kg:m <sup>2</sup> )	Moment of inertia of the 2nd arm around the center of gravity	0.117
$I_3$ (kg:m <sup>2</sup> )	Moment of inertia of 3rd arm around the center of gravity	0.535
$C_1$ (N:m:s)	Coefficient of viscous friction of the 1st hinge	0.0654
$C_2$ (N:m:s)	Coefficient of viscous friction of the 2nd hinge	0.0232
$C_3$ (N:m:s)	Coefficient of viscous friction of the 3rd hinge	0.0088
$\varphi_1$ (V/rad)	Gain of the 1st potentiometer	1.146
$\varphi_2$ (V/rad)	Gain of the 2nd potentiometer	1.146
$\varphi_3$ (V/rad)	Gain of the 3rd potentiometer	0.9964
$C_{m1}$ (N:m:s)	Viscous friction coefficient of the 1st motor	0.0022
$C_{m2}$ (N:m:s)	Viscous friction coefficient of the 2nd motor	0.0007

where  $F_L(P, K)(j\omega)$  represents the lower linear fractional transformation of the augmented plant  $P$  with controller  $K$ . Meeting this condition guarantees robust performance of the closed-loop system despite the presence of uncertainties. The  $\mu$ -synthesis procedure is implemented using the MATLAB function `dkfsyn`.

### III. SIMULATION RESULTS

The performance of the proposed control strategies was evaluated through extensive simulations using MATLAB. The  $H_\infty$  control design for the triple inverted pendulum was first implemented on the nominal model. The transient response under a reference input vector

$$r = [0 \quad -0.1 \quad 0.2]^T$$

is depicted in Figs. 2 and 3. These figures illustrate that the  $H_\infty$  controller achieves fast reference tracking with minimal overshoot in the output variables. Although the steady-state errors are negligible for most outputs, a slight error is observed in the position of the first arm.

In addition to reference tracking, the disturbance rejection capability of the  $H_\infty$  controller was examined. A disturbance vector

$$d = [0.1 \quad 0.1 \quad 0.1]^T$$

was introduced, and the corresponding closed-loop responses are presented in Figs. 4 and 5. The results indicate that the  $H_\infty$  controller effectively attenuates the disturbances while maintaining overall system stability.

Robust performance under uncertainty was further analyzed through the evaluation of the structured singular value. Fig. 6 shows the singular value plot of the uncertain model when the  $H_\infty$  controller is applied. This plot, obtained for various values of the uncertainty parameters, reveals that peaks in

the magnitude response can lead to potential instability in the closed-loop system if not adequately addressed.

To assess the worst-case performance, the uncertain model was simulated under adverse conditions. Figs. 7, 8, and 9 display the transient and disturbance responses for these worst-case scenarios. Despite the increased uncertainty, the  $H_\infty$  controller manages to maintain acceptable performance, albeit with some degradation compared to the nominal model.

For comparative purposes, the performance of a  $\mu$ -synthesis controller was also investigated. Figs. 10 and 11 illustrate the transient responses of the nominal closed-loop system using the  $\mu$ -controller. Although the reference tracking and disturbance rejection responses are slightly slower with the  $\mu$ -controller, this trade-off is necessary to ensure robust stability and performance over a wider range of operating conditions.

In summary, the simulation results validate the effectiveness of both control strategies. The  $H_\infty$  controller demonstrates superior transient performance and minimal steady-state error for the nominal model, while the  $\mu$ -synthesis controller offers enhanced robustness in the presence of uncertainties. These findings highlight the trade-offs between rapid response and robust performance, providing valuable insights into the controller selection process for complex dynamical systems.

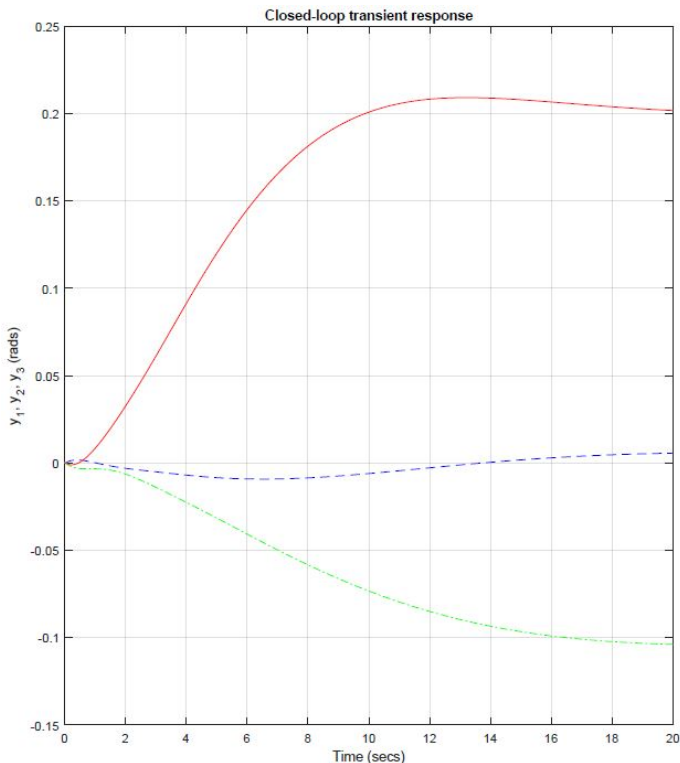


Fig. 2: Closed-loop transient responses ( $H_\infty$  controller)

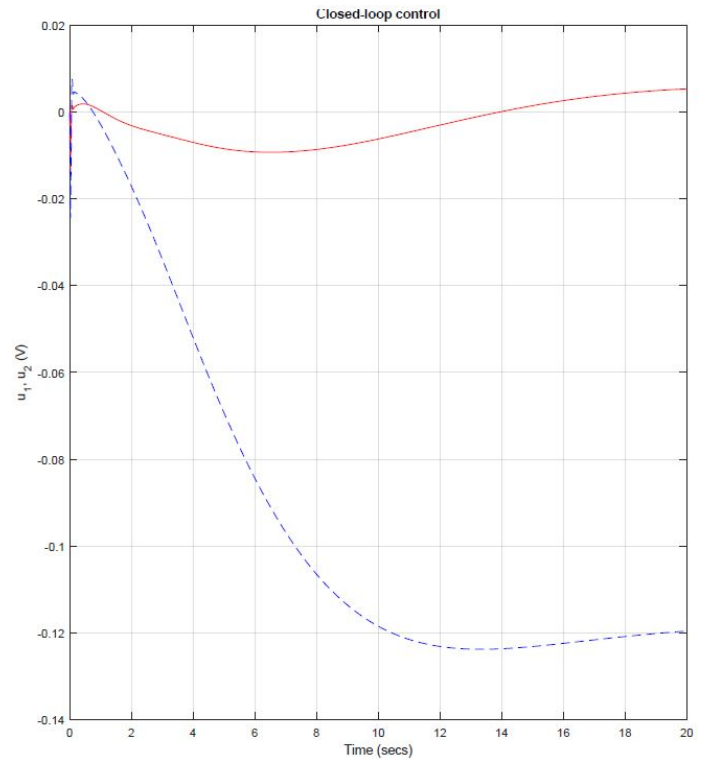


Fig. 3: Closed-loop control for reference tracking ( $H_\infty$  controller)

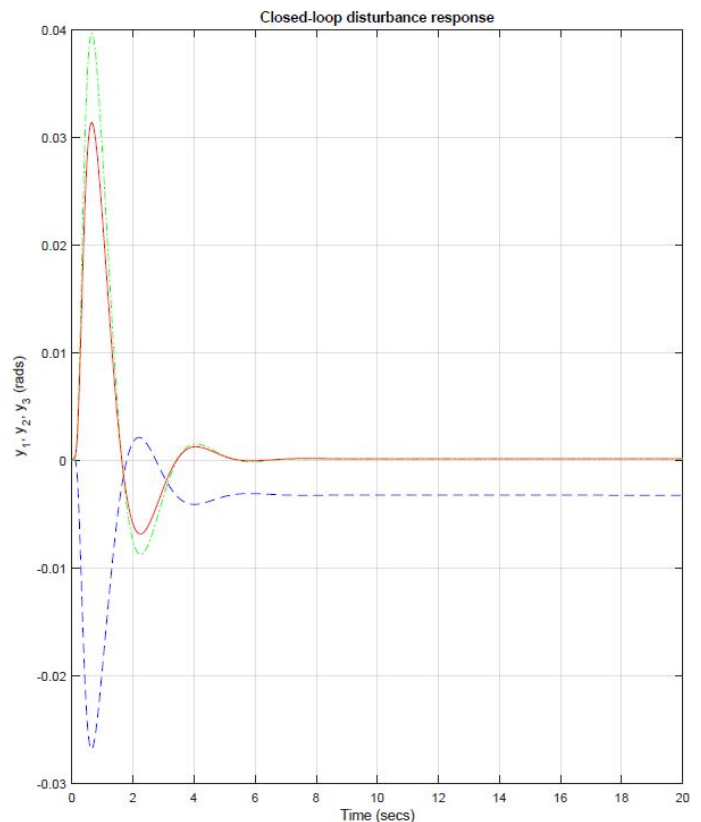


Fig. 4: Closed-loop disturbance responses ( $H_\infty$  controller)

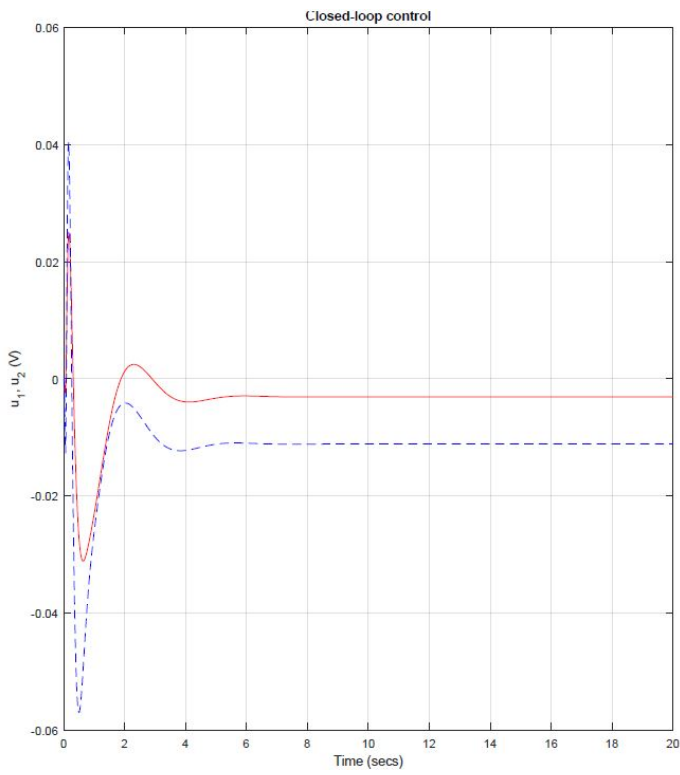


Fig. 5: Closed-loop control for disturbance rejection ( $H_\infty$  controller)

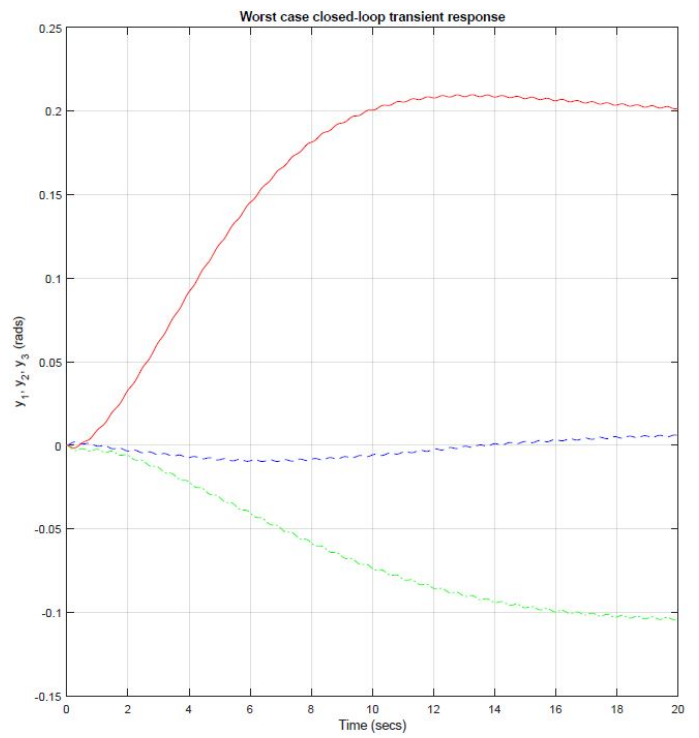


Fig. 7: Worst case closed-loop transient responses ( $H_\infty$  controller)

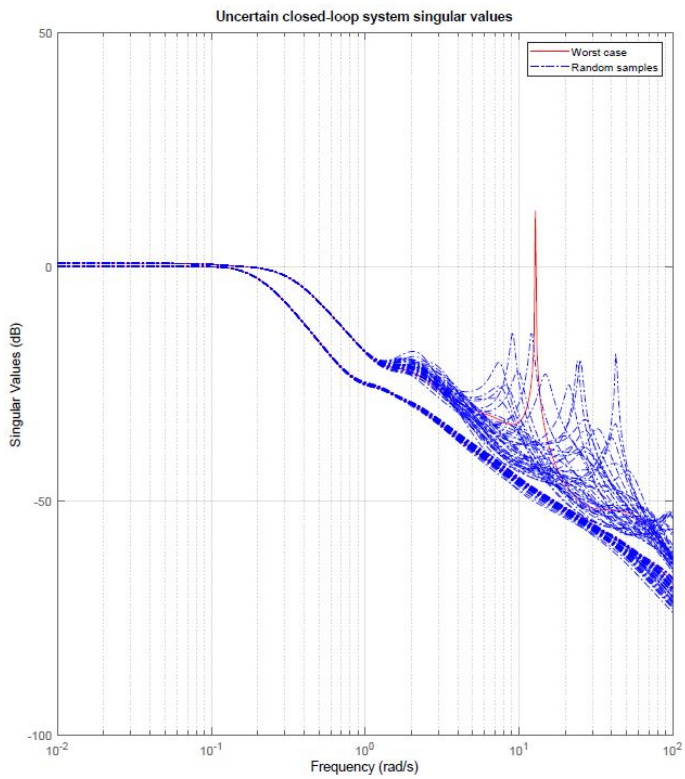


Fig. 6: Closed-loop singular values ( $H_\infty$  controller)

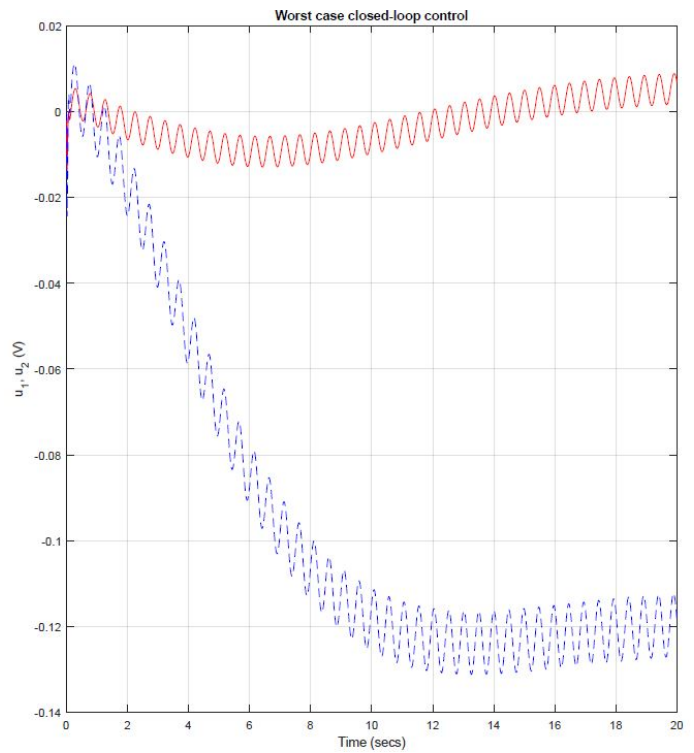


Fig. 8: Worst case closed-loop control for reference tracking ( $H_\infty$  controller)

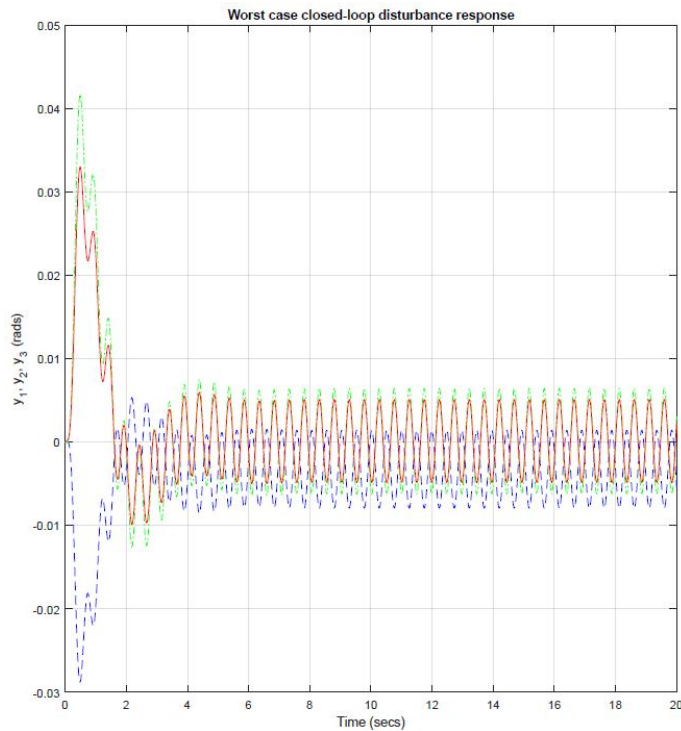


Fig. 9: Worst case closed-loop disturbance responses ( $H_\infty$  controller)

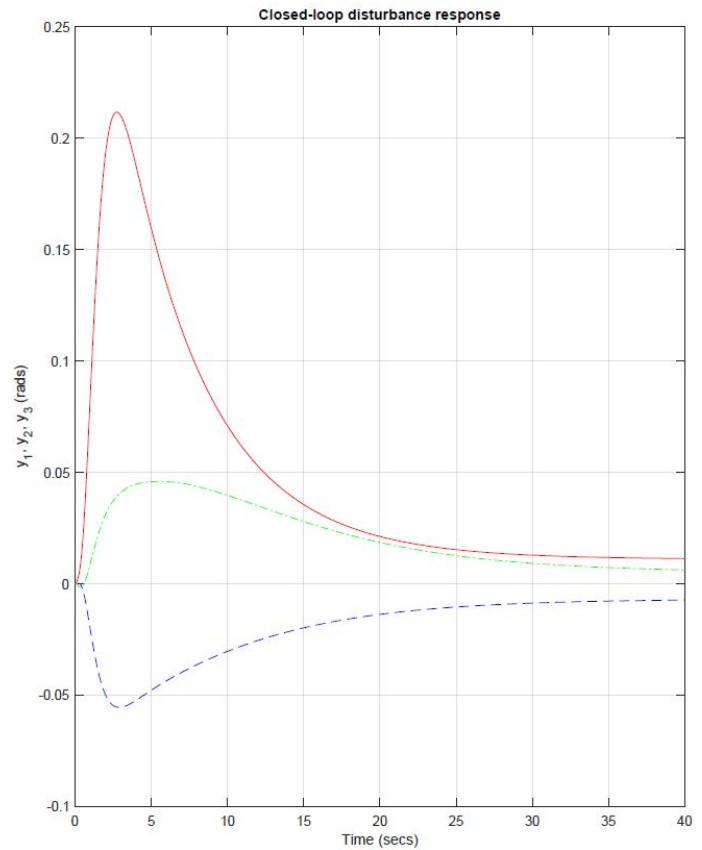


Fig. 11: closed-loop disturbance responses ( $\mu$ -controller)

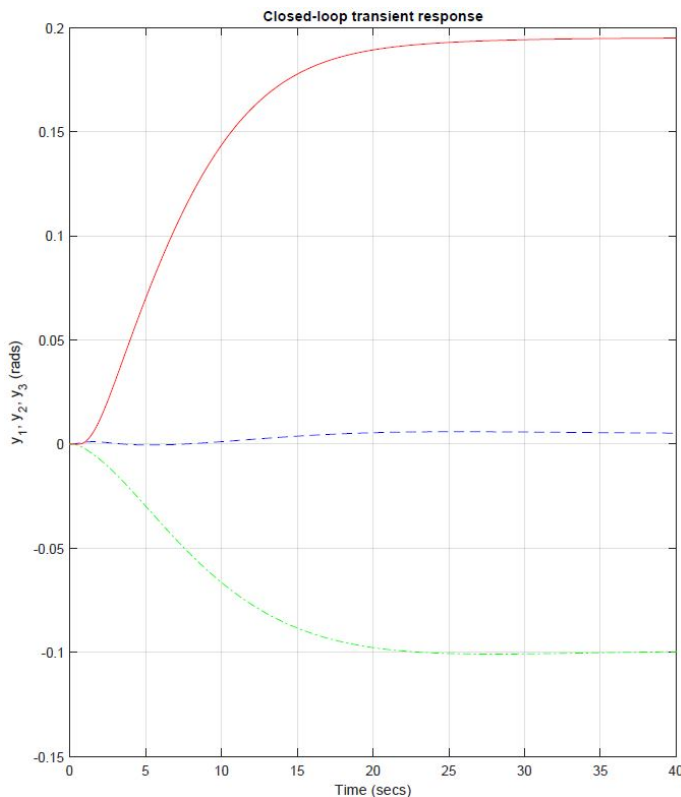


Fig. 10: Closed-loop transient responses ( $\mu$ -controller)

#### IV. CONCLUSION

In this paper, we presented robust control strategies for the stabilization of a triple inverted pendulum system. Both  $H_\infty$  and  $\mu$ -synthesis controllers were designed and implemented to address the challenges posed by the system's inherent nonlinearities and parameter uncertainties. Simulation results for the nominal model demonstrated that the  $H_\infty$  controller achieves fast reference tracking with minimal overshoot and effective disturbance rejection. Furthermore, the analysis of the structured singular value provided insight into the robust performance limitations under varying uncertainty levels. Although the  $\mu$ -synthesis controller exhibited slightly slower transient responses, it offers enhanced robustness over a broader range of operating conditions, which is essential for practical applications. Future work will focus on experimental validation of the proposed methods and the further exploration of adaptive control techniques to improve performance in the presence of time-varying uncertainties.

#### REFERENCES

- [1] J. Yi, N. Yubazaki, and K. Hirota, "A new fuzzy controller for stabilization of parallel-type double inverted pendulum system," *Fuzzy Sets Syst.*, vol. 126, no. 1, pp. 105–119, 2002.
- [2] S. Sehgal and S. Tiwari, "LQR control for stabilizing triple link inverted pendulum system," in *Proc. 2012 2nd Int. Conf. Power, Control and Embedded Systems*, 2012.
- [3] K. Furut, T. Ochiai, and N. Ono, "Attitude control of a triple inverted pendulum," *Int. J. Control*, vol. 39, no. 6, pp. 1351–1365, 1984.

- [4] H. Meier Farwig, H. Zu, and H. Unbehauen, "Discrete computer control of a triple-inverted pendulum," *Optimal Control Appl. Methods*, vol. 11, no. 2, pp. 157–171, 1990.
- [5] X. Li, M. Zhe, and W. Xiaolin, "Comparative study on H1 robust control based on dynamic state feedback and static state feedback," in *Proc. 2017 29th Chinese Control and Decision Conference (CCDC)*, 2017.
- [6] K. Furut, T. Ochiai, and N. Ono, "Attitude control of a triple inverted pendulum," *Int. J. Control*, vol. 39, no. 6, pp. 1351–1365, 1984.
- [7] T. Kargar Tasooji and H. J. Marquez, "Cooperative Localization in Mobile Robots Using Event-Triggered Mechanism: Theory and Experiments," in *IEEE Transactions on Automation Science and Engineering*, vol. 19, no. 4, pp. 3246–3258, Oct. 2022, doi: 10.1109/TASE.2021.3115770.
- [8] T. K. Tasooji and H. J. Marquez, "Event-Triggered Consensus Control for Multirobot Systems With Cooperative Localization," in *IEEE Transactions on Industrial Electronics*, vol. 70, no. 6, pp. 5982–5993, June 2023, doi: 10.1109/TIE.2022.3192673.
- [9] T. K. Tasooji, S. Khodadadi and H. J. Marquez, "Event-Based Secure Consensus Control for Multirobot Systems With Cooperative Localization Against DoS Attacks," in *IEEE/ASME Transactions on Mechatronics*, vol. 29, no. 1, pp. 715–729, Feb. 2024, doi: 10.1109/TMECH.2023.3270819.
- [10] T. K. Tasooji and H. J. Marquez, "Decentralized Event-Triggered Cooperative Localization in Multirobot Systems Under Random Delays: With/Without Timestamps Mechanism," in *IEEE/ASME Transactions on Mechatronics*, vol. 28, no. 1, pp. 555–567, Feb. 2023, doi: 10.1109/TMECH.2022.3203439.
- [11] T. Kargar Tasooji and H. J. Marquez, "A Secure Decentralized Event-Triggered Cooperative Localization in Multi-Robot Systems Under Cyber Attack," in *IEEE Access*, vol. 10, pp. 128101–128121, 2022, doi: 10.1109/ACCESS.2022.3227076.
- [12] S. Khodadadi, T. K. Tasooji and H. J. Marquez, "Observer-Based Secure Control for Vehicular Platooning Under DoS Attacks," in *IEEE Access*, vol. 11, pp. 20542–20552, 2023, doi: 10.1109/ACCESS.2023.3250398.
- [13] M. A. Gozukucuk et al., "Design and Simulation of an Optimal Energy Management Strategy for Plug-In Electric Vehicles," 2018 6th International Conference on Control Engineering & Information Technology (CEIT), Istanbul, Turkey, 2018, pp. 1–6, doi: 10.1109/CEIT.2018.8751923.
- [14] A. Mostafazadeh, T. K. Tasooji, M. Sahin and O. Usta, "Voltage control of PV-FC-battery-wind turbine for stand-alone hybrid system based on fuzzy logic controller," 2017 10th International Conference on Electrical and Electronics Engineering (ELECO), Bursa, Turkey, 2017, pp. 170–174.
- [15] T. K. Tasooji, A. Mostafazadeh and O. Usta, "Model predictive controller as a robust algorithm for maximum power point tracking," 2017 10th International Conference on Electrical and Electronics Engineering (ELECO), Bursa, Turkey, 2017, pp. 175–179.
- [16] T. K. Tasooji, O. Bebek, B. Ugurlu, "A Robust Torque Controller for Series Elastic Actuators: Model Predictive Control with a Disturbance Observer" Turkish National Conference on Automatic Control (TOK), Istanbul, Turkey pp. 398–402, 2017
- [17] T. K. Tasooji, "Energy consumption modeling and optimization of speed profile for plug-in electric vehicles", M.Sc. dissertation, Ozyegin Univ, Istanbul, Turkey, 2018
- [18] T. K. Tasooji, "Cooperative Localization and Control In Multi-Robot Systems With Event-Triggered Mechanism: Theory and Experiments", Ph.D. dissertation, Univ. Alberta, Edmonton, AB, Canada, 2023
- [19] S. Khodadadi, "Observer-Based Secure Control of Vehicular Platooning Under DoS attacks", M.Sc. dissertation, Univ. Alberta, Edmonton, AB, Canada, 2022
- [20] A. Sagale, T. K. Tasooji, and R. Parasuraman, "DCL-sparse: Distributed range-only cooperative localization of multi-robots in noisy and sparse sensing graphs," arXiv [cs.RO], 2024.
- [21] T. K. Tasooji, S. Khodadadi, G. Liu, R. Wang, "Cooperative Control of Multi-Quadrotors for Transporting Cable-Suspended Payloads: Obstacle-Aware Planning and Event-Based Nonlinear Model Predictive Control", arXiv:2503.19135v1 [cs.RO]